Polarization Properties of Atmospheric Cerenkov Pulses

A.K. Tickoo[1], **M.Kothari**[1], **H.C. Goyal**[1], **V.K. Dhar**[1], **R. Koul**[1], **S.K. Kaul**[1], **R.C. Rannot**[1], **R.K. Kaul**[1], **A. Haungs**[2], **H. Rebel**[2] **and C.L. Bhat**[1]
[1]*Bhabha Atomic Research Centre, Nuclear Research Laboratory, Trombay, Mumbai-400085, India*
[2]*Forschungszentrum, Karlsruhe, IK3 D-76021, Karlsruhe, Germany*

Abstract

We present here first results from an on-going experiment set up to measure the polarization state (degree and angle of linear polarization) of atmospheric Cerenkov pulses, produced by (mainly) cosmic-ray primaries of energy $\geq$ 4 PeV. The inferred degree of linear polarization averages to $\sim 40\%$ and appears to have a rather weak dependance on the shower-core distance. The interesting possibility of using two or more independent measurements of the polarization angle, for the same event, for estimating its core location is also discussed.

1 Introduction:

A ‘first-principles’ understanding of the physics of Cerenkov radiation and the processes involved in the Extensive Air-Shower (EAS) development suggests that the accompanying atmospheric Cerenkov light, detected at the ground level, may be significantly polarized (Jelley; 1967). Furthermore, as a good fraction of the Cerenkov light is produced near the EAS core, in general, the projection of the electric vector of the detected Cerenkov photon ($\sim$ polarization direction) should point in the direction in which the shower core would impact the ground. In such a case, the polarization state of an Atmospheric Cerenkov Event (ACE) may provide two additional parameters, viz., degree (p) and angle (θ) of polarization, for a supplementary characterization of the progenitor particle — an important problem receiving a lot of attention these days (Haungs et al; 1999). In addition, the angle -parameter (θ), when measured at two or more places in a correlated manner, may provide an independent estimate of the EAS core-location.

There is hardly any guidance available from the published literature on this interesting subject. The first experimental work by Galbraith and Jelley (1955), using a simple Cerenkov light collector operated in combination with a linear array of Geiger counters, has produced only some tentative results. The general thrust of this work seems to be in a qualitative agreement with the above-referred anticipation about the general polarization state of the ACE. Similarly, EAS simulation studies, carried out more recently by Hillas (1996) and Bhat et al (1999), using γ-ray and proton-progenitors in the TeV energy range, suggest that the average degree of polarization, $<$p$>$, increases gradually between 5 - 45% for γ-rays and lies between $\sim 15 - 25\%$ for protons over the core distance range, R $\sim$ 0 - 140m, beyond which $<p>$ remains at $\sim 20\%$ for either species for 140 m $< R <$ 200m. In view of the implied characterization potential of the polarization feature of the ACE and the fact that no quantitative measurements have been carried out so far on this important intrinsic property of the atmospheric Cerenkov light, we have undertaken to do so using the prototype MYSTIQUE array (pro-MYST), recently set up Mt. Abu (24.62^o N, 72.75^o E, 1275m asl) in Rajasthan, Western India. In what follows, we describe the pro-MYST experimental arrangement and discuss the first results obtained from this exploratory investigation.

2 PRO-MYST Experiment:

Fig.1a gives a schematic representation of the pro-MYST array. It comprises photomultiplier tube (PMT, type RCA 8575)-based, 12 vertically-oriented, wide FoV (45^o half-angle) detector elements which are spread out over a geographical area of $\sim 3500 m^2$. One of these is the Central Element (CE), which is surrounded by 8 Timing Elements (TE 1-8) with the nearest-neighbour distance of $\sim$ 50m from one another. In addition, there are 3 Polarization Elements, labelled PE 2, 5 and 8 since they are placed in the physical proximity of the TE 2, 5 and 8 respectively. The CE consists of 3 PMT channels which are operated in a prompt, 3 fold-coincidence mode (resolving time $\sim$ 10ns), while each TE deploys 2 PMT, again operated in a similar 2-fold fast-coincidence mode (see Fig.1b for details of the system electronics). Each PE comprises 3 PMT, which have sheet polaroids (type HNB P-UV2) mounted near their photocathode surfaces with their polarization axes mutually displaced by 120^o (all angles measured w.r.t. geographical North-South line). Whenever the CE produces a 3-fold prompt trigger, the Equivalent Photo-Electron Counts (EPEC) of the associated event, as detected by each of the 28 PMT channels belonging to the CE, TE and PE, are registered. To ensure a proper time-synchronization, the 3 Charge-to-Digital Converter (CDC) channels, connected to the CE amplifier outputs are gated by the CE-generated 3-fold trigger pulse, while the CDC channels of each TE and the neighbouring PE (in case of TE 2,5 and 8) are prompted by the 2-fold trigger output of the related TE itself, as shown in Fig.1(b). The relative arrival times of the event at various TE channels w.r.t. the occurrence time of the CE master trigger are logged in 8 Time-to-Digital Converter (TDC) channels, using a time resolution of 0.25 ns and a full-scale value of 500 ns. These TDC data help to reconstruct the arrival direction of the recorded ACE, using an appropriate atmospheric Cerenkov wavefront-fitting procedure.

It has been possible to provide an absolute calibration for each of the 28 PMT channels in an off-line manner (i.e., when no observations are taking place), using a combination of the single-photoelectron counting technique and an Am^{241} pulsed light source. Each light pulse from the pulser is found to correspond to 1500 EPEC. During actual observations, each PMT channel is operated at the same EHT on a night-to-night basis. The d.c. anode current of each PMT, while exposed to the night sky, is monitored on an hourly basis to ensure a PMT gain stability of within $\pm$ 15% throughout the observations. The hardware discrimination level of 150 mV, preset for the CE and TE channels, corresponds to 10 EPEC. The pro-MYST event trigger-rate turns out to be 4.7 $\min^{-1}$, corresponding to a nominal cosmic-ray primary energy $\geq$ 800TeV. An overall data-sample of 53900 events, collected in 190 h of observations on clear, moonless nights between November 1998 to March 1999, is used in the present work.

3 Data Analysis and Results:

Assuming that a uniform light flux I_o is incident on each of the 3 detector channels of a PE, the degree of linear polarization, p, and angle of polarization, θ, is related to the light fluxes I_i (i = 1-3), actually detected by the 3 channels, by (Sen et al. 1990):

$$p = \frac{2\sqrt{I_1(I_1-I_2)+I_2(I_2-I_3)+I_3(I_3-I_1)}}{I_1+I_2+I_3} \tag{1}$$

$$\theta = \frac{1}{2}tan^{-1}\frac{\sqrt{3}(I_3-I_2)}{(2I_1-I_2-I_3)} \tag{2}$$

Using, in place of I_i (i=1-3), the EPEC recorded by a given PE channel in response to an ACE registration by the pro-MYST, Equations (1) & (2) have been solved for calculating p and θ for each such event. But, as is implicit in the application of these equations, it has been ensured first that the light flux (I_o), incident on the 3 PMT channels of a PE from an ACE, are comparable. For this purpose, we have estimated the EPEC ratio for the two PMT channels of the corresponding TE and, reassuringly find it to have a peak value of 1 (1 standard deviation =0.25) for all the recorded ACE. Fig. 2a gives the resulting frequency distribution of p for all the 'single' PE data, i.e., events which are detected by only one of the 3 PE (in addition to the CE). This figure is based on 'robust' ACE for which the EPEC $\geq$ 100 in either channel of a TE and is $\geq$ 30 for each of the 3 channels of the corresponding PE. The inferred degree of polarization is found to vary between 5-95 % on an event-to-event basis with a mean value $< p > \sim$ 40 %. All the 3 PE data, taken individually, are found to conform to the global picture of Fig. 2a. On the other hand, the angle of polarization, derived for each PE, is found to cover all θ between $\sim$ 0 - 360^o, with a peaking tendency in two directions. This is evident from the representative polar diagram of Fig. 2b giving θ distribution for ACE as recorded by PE-5. Assuming that θ is indeed in the direction of the point of impact of the EAS core on the ground, the observed angular distribution, with 2 wings 180^o apart, can be mainly attributed to geometrical effects, viz., that an ACE, has a finite 'circle of influence' around the core position, consistent with the lateral distribution of atmospheric Cerenkov light and has to be detected by one of the 3 PE, in addition to the CE.

Following the line of argument outlined in the Introducion, for the ACE 'seen' by $\geq$ 2 PE, it is possible to infer the position of the EAS core by finding the point(s) of intersection of the polarization vectors from 2(3) PE. In the 2 PE case, we can thus get one such core-location, without any estimate of the corresponding error. In the case where all the 3 PE respond to an ACE and yield 3 independent (p, θ) pairs, there can be upto 3 points of intersection. The core distance in this case may be taken as the distance R_o to the centroid of the triangle formed by these 3 points and the error in the core distance, as ΔR_o = 1/3 $\sum_{i=1}^{3} |R_i - R_o|$, where R_i is the corresponding distance to the ith vertex. Defined thus, Fig. 3 gives the distribution of the core-positions relative to CE and PE locations, as inferred for the events which are detected by any 2 of the 3 PE. An examination of the figure reveals a noticeable clustering of the inferred core-locations in 3 circular sectors at distances of $\sim$ 65 m from the CE. As mentioned above in the case of 1 PE events, this concentration of the core positions for 2 PE events is a geometrical effect, resulting from the fact that each core has a 'circle of influence' of finite radius around it. Simulations indicate this radius to be $\sim$ 100 m for events shown in Fig.3, consistent with the lateral distribution of the Cerenkov pool and the relatively high EPEC threshold values (30) used for the PE channels.The core -location distribution noted for 3 PE events (81 in number) is also found to be in good general agreement with these geometrical considerations.

The overall good agreement noted between the observed and expected core distributions for 2 PE and 3 PE events suggests that, at least in a statistical sense, the polarization technique yields reliable information about the EAS core location. What will need to be established now is the validity of this independent core-estimation procedure on an event-by-event basis, a task presently in progress. In the meanwhile, taking the polarization-derived core distance (R) at its face value, we show in Fig.4, a plot of p versus R for the 2 PE and 3 PE events together. The results are seen to be consistent with the picture obtained from Fig.2a (1 PE events) as far the average degree of polarization and the event-to-event variations in this value. No significant dependence of $<$ p $>$ is indicated on the core distance in the case of (predominantly cosmic-ray generated) events, detected by the pro-MYST. Following the prescription outlined above, the error in the inferred-core location R for the 3 PE events is found to vary widely with a mean value of $\sim 35-45\%$ over R $\sim$ 25-150m. More statistics is required to make this inference firmer.

4 Conclusions:

First systematic experimental evidence is presented here establishing that the ACE generated by the cosmic-ray with a primary energy $\geq$ 4 PeV, are linearly polarized with an average value $\sim 40\%$ for the degree of polarization. It is also indicated that the polarization-angle information can, in principle, be useful in providing an independent estimate of the core distance. The average degree of polarization in case of cosmic-ray generated ACE is seen to be not particularly sensitive to the shower-core distance. It would be of great interest to find the corresponding situation for γ-ray generated ACE in order to assess the potential of this technique for supplementary event characterization purposes.

References

Bhat, C.L., et al, 1999, To appear in Bull. Astr. Soc. of India

Galbraith, W and Jelley, J.V., 1955, Journal of Atmospheric and Terrestrial Physics, 6, 250

Jelley, J.V, 1967, Progress in Cosmic rays and Elementary Particle Physics, 9

Haungs, A., et al, 1999, Astrop. Phys. (in press)

Hillas, A.M., 1996, Space Science Reviews, 75, 17

Sen, A.K., et al, 1990, ICARUS, 86, 248

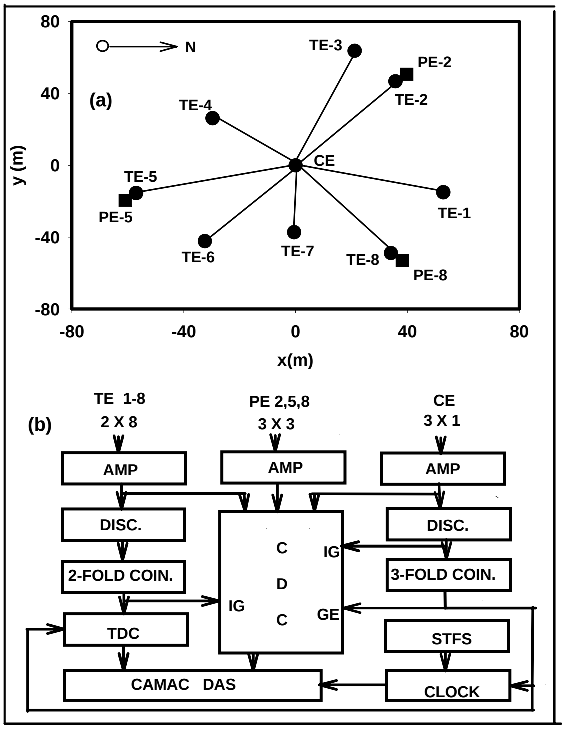

Figure 1: (a) Pro-MYST array detector layout. (b) Instrumentation block diagram. Labels used are; IG : Individual Gate, GE : Gate Enable. Delay cables (not shown) are used for proper time synchronization.

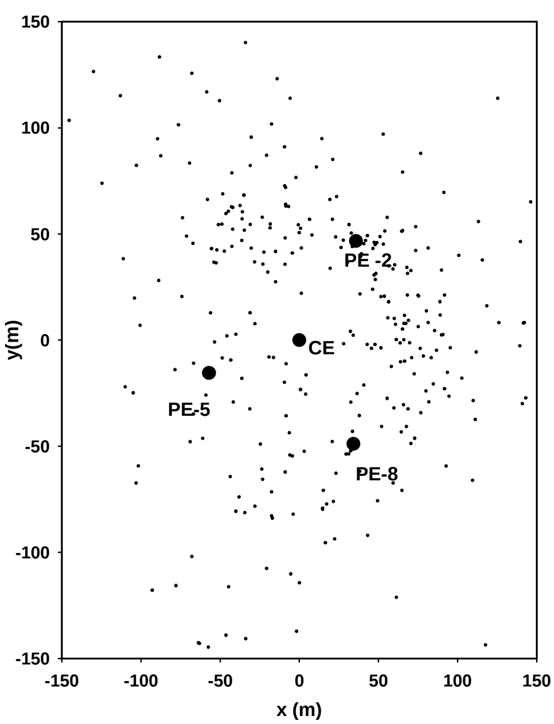

Figure 3: Distribution of inferred core-locations relative to CE and PE positions for events detected by 2 PE (in addition to CE).

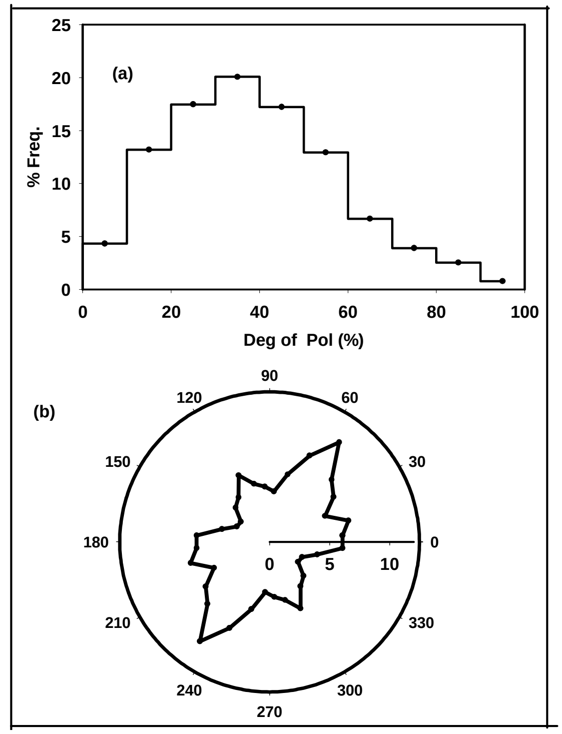

Figure 2: (a) Frequency distribution of inferred degree of polarization (p) for events detected by either PE-2 , PE-5 or PE-8, in addition to CE. (b) Representative polar diagram of angle of polarization (θ) for events detected by PE-5 (in addition to CE). Radial scale represents number of detected events (in %).

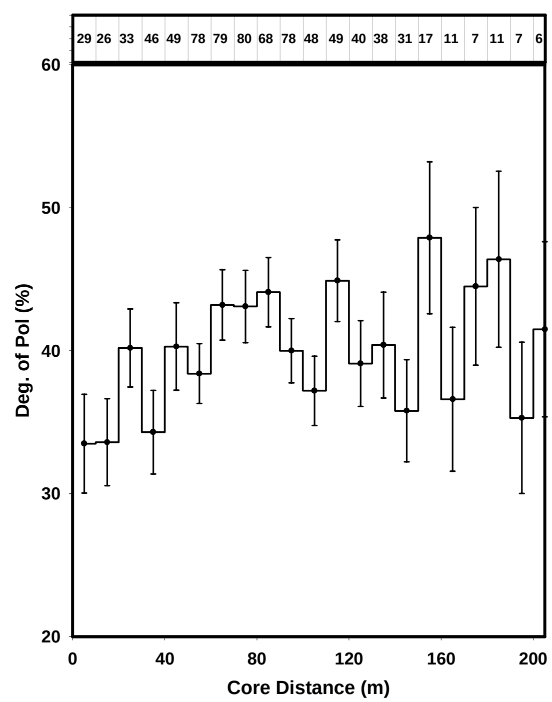

Figure 4: Average degree of polarization versus deduced core distance for 2PE and 3PE events. Error bars represent standard error values calculated for event numbers listed at the top of the